Factors affecting the estimate of primary production from space

W. M. Balch and C. F. Byrne

Division of Marine Biology and Fisheries, Rosenstiel School of Marine and Atmospheric Science
University of Miami, Miami, Florida

Abstract. Remote sensing of primary production in the euphotic zone has been based mostly on visible-band water-leaving radiance measured with the coastal zone color scanner. There are some robust, simple relationships for calculating integral production based on surface measurements, but they also require knowledge of photoadaptive parameters such as maximum photosynthesis which currently cannot be obtained from space. A 17,000-station data set is used to show that space-based estimates of maximum photosynthesis could improve predictions of Ψ, the water column light utilization index, which is an important term in many primary productivity models. Temperature is also examined as a factor for predicting hydrographic structure and primary production. A simple model is used to relate temperature and maximum photosynthesis; the model incorporates (1) the positive relationship between maximum photosynthesis and temperature and (2) the strongly negative relationship between temperature and nitrate in the ocean (which directly affects maximum growth rates via nitrogen limitation). Since these two factors relate to carbon and nitrogen, "balanced carbon/nitrogen assimilation" was calculated assuming the Redfield ratio. It is expected that the relationship between maximum balanced carbon assimilation versus temperature is concave-down, with the peak dependent on nitrate uptake kinetics, temperature-nitrate relationships, and the carbon/chlorophyll ratio. These predictions were compared with sea truth data. The minimum turnover time for nitrate was also calculated using this approach. Lastly, sea surface temperature gradients were used to predict the slope of isotherms (a proxy for the slope of isopycnals in many waters). Sea truth data show that at size scales of several hundred kilometers, surface temperature gradients can provide information on the slope of isotherms in the top 200 m of the water column. This is directly relevant to the supply of nutrients into the surface mixed layer, which is useful for predicting integral biomass and primary production.

Introduction

The Problem

The fundamental difficulty in estimating primary productivity from satellite-derived pigments is that an indicator of standing stock (phytoplankton pigment) is being used to calculate a rate (carbon fixation). The fact that chlorophyll and photosynthesis are not always well correlated has been understood since the early days of the ^{14}C method [*Steeman Nielson*, 1963], when the only way to relate a rate from a standing stock was to add information about the supply rate of some limiting factor such as quanta or nutrients [e.g., *Blackman*, 1905; *Riley*, 1946]. Surprisingly, we are still faced with this problem in the determination of primary production from space, and several issues need to be resolved. The first has been the prediction of subsurface biomass profiles, a major source of error in primary production algorithms. The coastal zone color scanner (CZCS) detected phytoplankton pigment 1 optical depth into the water (defined as the reciprocal of the diffuse attenuation coefficient at a given wavelength K_λ [*Gordon and McCluney*, 1975], whereas it is well known that phytoplankton can be photosynthetically active to 4.6 optical depths or more. In highly stratified situations, the satellite therefore "observed" as little as 5% of the total phytoplankton biomass. Models have therefore been used to predict subsurface biomass profiles based on surface pigment concentrations, ranging from purely empirical relations [*Smith et al.*, 1982; *Balch et al.*, 1989] to simple semianalytical relationships [*Smith et al.*, 1987; *Balch et al.*, 1992] or more elaborate semianalytical relationships that vary regionally [*Platt and Sathyendranath*, 1988; *Morel and Berthon*, 1989]. One comparison of empirical, simple semianalytical and more complex regional semianalytical approaches explained the same amount of variance in integral biomass for all cases when compared over 2000 stations of data [*Balch et al.*, 1992]. This result may have been due to data quality issues, since a wide variety of data sets were pooled for the analysis. Nevertheless, the striking result was that regardless of the approach, we were left with essentially the same degrees of freedom. The need for more information in calculating integral biomass is obvious.

Another way to relate satellite-derived algal biomass measurements to production rates involves information about the photon flux. In most cases investigators have used the fundamental relationship between light and photosynthesis, called a *P-I* curve [*Platt and Jassby*, 1976]. The formulation requires at least two photoadaptive parameters, α (the light-limited slope of the *P-I* curve) and P_m^b (the maximum photosynthetic rate per unit chlorophyll at light saturation). A third photoadaptive parameter I_k, the light intensity at which photosynthesis saturates, can be derived as P_m^b/α.

Paper number 93JC03091.
0148-0227/94/93JC-03091$05.00

Thus any two of the three photoadaptive parameters α, P_m^b, and I_k can be used to calculate the third and provide relatively complete information about the physiological response of phytoplankton to light. Photoinhibition [*Gallegos et al.*, 1983] may also be relevant for shade-adapted populations on a seasonal and latitudinal basis [*Harrison and Platt*, 1986]. Algorithms based on photoadaptive parameters hereafter will be referred to as *P-I* algorithms.

Interestingly, the first such *P-I* algorithms, produced three decades ago, are still in use today and give relatively good estimates of integral primary production as long as one knows the photoadaptive parameters. Given shipboard data for P_m^b, the simplest primary production models explained as much as 67% of the variance in integral primary production at 1754 stations [*Balch et al.*, 1992]. The more complex spectral-, time-, depth-resolved model of *Platt and Sathyendranath* [1988] explains 90% of the variance in integral production at about 30 stations when shipboard estimates of the photoadaptive parameters are used. When only data available to a satellite was used (i.e., the photoadaptive parameters are guessed), the explained variance for all models falls precipitously to 12–30% for predicting integral production [*Balch et al.*, 1992; *Balch*, 1993]. Such low accuracy frustrates attempts to acquire broad-scale estimates of carbon fixation using a satellite.

Lastly, there is the issue of how to interpret production estimates from space. Satellite-derived estimates of primary production based on *P-I* algorithms may not have much to do with changes in algal biomass observed in satellite images. Most "loss terms" are excluded in bottles. Usually, researchers screen out large grazers before incubating phytoplankton in bottles, leaving microzooplankton in. Once the water is in the bottle, losses due to sinking, advection, and diffusion disappear. Sinking is probably the least important loss term, especially in oligotrophic environments, where small, slowly sinking picoplankton dominate. While most ^{14}C incorporation in bottle experiments is due to photosynthesis, it is not possible to say whether an increase in phytoplankton biomass in a satellite image is due to a change in the chlorophyll distribution, the algae growing more, their being grazed less, or a decrease in their C/chlorophyll ratio. Such information is critical to understanding the rates of turnover of carbon in the euphotic zone. Time-dependent factors also affect primary production estimates. For example, the assimilation number likely will vary between early and late stages of an algal bloom as nutrient concentrations change, and metabolic rates will shift up and down accordingly [*Wilkerson and Dugdale*, 1987; *Dugdale and Wilkerson*, 1989]. Without satellite access to photoadaptive parameters, it is difficult to derive primary production from knowledge of just pigment and light fields. Since balanced growth requires knowledge of both carbon and nitrogen assimilation rates, nutrient supply rate remains a key area to examine for the remote sensing of phytoplankton production. This is not a new concept, given the comment by *Steeman Nielsen* [1963, p. 135]: "Present knowledge of primary production in the ocean has shown an exceedingly remarkable correlation with hydrographic conditions."

Temperature as an Indicator of Nutrient Supply

Temperature can provide information about the nitrate concentration in seawater and the potential for new production. For most water masses the relation between temperature and nitrate is best defined at moderate to low seawater temperatures and breaks down at higher seawater temperatures. For example, in the Southern California Bight and other regions of its latitude, nitrate concentrations linearly decrease to undetectable levels between 0° and 15°C and then remain undetectable above 15°C [*Kamykowski*, 1973; *Zentara and Kamykowski*, 1977; *Jackson*, 1983]. Thus as long as sea surface temperature (SST) is less than 15°C in the Southern California Bight, one can use it to roughly estimate surface nitrate concentrations. SST not only indicates the standing stock of nitrate but also may provide insight into the rate of nitrate utilization. *Dugdale et al.* [1989] estimated new production using remotely sensed temperature and color and a shift-up model for growth on nitrate. *Campbell and Aarup* [1992] have calculated new production in the North Atlantic based on the initial deepwater nitrate values, the rate of thermocline erosion, and the stoichiometric conversion of pigment to particulate nitrogen as the spring bloom forms and decays. *Sathyendranath et al.* [1991] also made a satellite-based estimate of new production over Georges Bank by relating SST to nitrate concentrations and then using the nitrate to calculate the "*f* ratio" (ratio of primary production based on allochthonous nutrients to total primary production [*Eppley and Peterson*, 1979]. Thus it appears likely that SST can provide information for the calculation of surface nitrate concentrations. If there is indeed a well-defined relationship between nitrate concentration and the *f* ratio, then SST will be useful for calculating new production from satellites.

Temperature Constraints on Physiology and Growth

Another, more physiological effect of temperature is its relation to enzyme-dependent reactions of photosynthesis. There is an extensive literature on the effects of temperature on photosynthesis [see *Talling*, 1955; *Berry and Bjorkman*, 1980; *Li*, 1980; *Geider*, 1987; *Davison*, 1991], but generally, temperature has not been thought to be the major factor affecting suboptimal photosynthetic rates at low and midlatitudes. There is evidence from high-latitude populations that I_k, the light level at which photosynthesis saturates, and I_m, the optimum light level for photosynthesis, are strongly temperature dependent [*Harrison and Platt*, 1986]. The relationship between the maximum carbon-specific growth rate of cultured phytoplankton versus temperature is a distinctly positive, exponential curve [*Eppley*, 1972]. The cultures used in Eppley's analysis were all examined under nutrient-replete conditions where temperature was rate limiting. Assuming a constant carbon:chlorophyll ratio, this curve sets the upper limits to photosynthetic rates, which are often saturated in the upper reaches of the water column visible to the satellite. However, suboptimal photosynthesis estimates in nature likely result from limiting light and nutrients (see his Figure 1), obscuring the relationship between production and temperature.

Balanced growth occurs when elemental constituents of algal tissue increase exponentially and at the same rate [*Shuter*, 1979]. For example, balanced growth in the ocean for carbon and nitrogen would occur when the carbon-specific and nitrogen-specific growth rates were equal. This is unlikely in nature at time scales of <24 hours, since the supply of photons is not continuous; when averaged over longer time scales, balanced growth is still unlikely, given that nitrogen is frequently limiting and the average ratio of

nitrogen to phosphorous in particulate matter is 16 while that in seawater is 15 [*Redfield et al.*, 1963]. It would follow that if growth was balanced in the cultures described by *Eppley* [1972], then maximum nitrogen-specific growth should also be an exponentially increasing function of temperature. While this interpretation is compelling, there is reason to believe that in the ocean, the relationship is more complex. This is so because nitrate availability in the ocean is a strongly negative function of temperature. Therefore to understand the effect of temperature on C/N balanced growth, the Eppley growth curve needs to be combined with the curves describing nitrate concentration versus temperature and nitrogen-specific growth versus nitrate concentration.

Remote sensing of phytoplankton growth requires that algorithms incorporate information both on the rate of supply of quanta and on the supply of nitrogen to the euphotic zone. Algorithms that deal with only one of these factors would be expected to be limited in their predictive ability, at least for estimating balanced growth. The problem remains of how we can understand the supply rate of nitrate through the base of the euphotic zone if satellite sensors "see" only several meters into the water column in the visible bands and several centimeters in the infrared. There may be a solution to this problem provided (1) that the sea surface temperature is related to the temperature of the upper water column and (2) that the density field is mostly influenced by temperature, not salinity. Under these conditions a transect into colder surface water will be associated with shoaling isotherms and isopycnals. In other words, measurements that can be made from space, like the gradient in sea surface temperature, may relate to the slope of deeper isotherms and isopycnals (baroclinicity).

The objectives of this work all focus on ways to improve estimates of primary production from space. These objectives are (1) to elucidate the relationships between maximum photosynthesis, beam attenuation, surface irradiance and integral primary production; (2) to model the relationship between temperature and P_m^b in the ocean and compare it to sea truth data; and (3) to examine the gradient in sea surface temperature and see whether it could be used to estimate baroclinicity in the surface ocean.

Methods

The data used in this study were a compilation of many data sets of hydrographic, pigment, productivity, and nutrient observations (Table 1). Digitization of these data was described in an earlier work [*Balch et al.*, 1992]. Further data have been entered into the data set, and a map of the station locations is shown in Figure 1. The total data set consists of 17,461 stations. Calculation of the diffuse attenuation coefficient, conversion of all rates to the same time units ("per day," which required knowledge of day length), and integrations of all the pigment and productivity profiles was described by *Balch et al.* [1992]. We discovered an error in the documentation of the National Oceanographic Data Center (NODC) 029 data set which caused virtually all of the productivity values to be flagged and eliminated from subsequent analyses. An investigation of the original data reports at the University of Washington and University of Alaska verified a decimal point error such that the discrete productivity values were 2 orders of magnitude too large. Therefore the NODC 029 productivity data used in this paper have been divided by 100. Following conversion to similar units, the entire data set was searched for predictive indices of integral production and Ψ, the light-scaled, depth-integrated assimilation number [*Falkowski*, 1981].

Temperature-Growth Model

A model was used to predict the relationship between carbon assimilation and temperature, which includes the effect of temperature on nutrient availability. The equation of *Eppley* [1972] was used to calculate maximum carbon assimilation. First, the carbon-specific maximum growth rate (μ_{maxC} as doublings per day) was calculated:

$$\mu_{\text{maxC}} = 10^{((0.0275 \times T) - 0.07)} \quad (1)$$

where T was temperature in degrees Celsius. Then maximal carbon assimilation per unit chlorophyll (Chl) was calculated (ΔC/Chl in grams C per gram Chl per day):

$$\Delta\text{C/Chl} = \text{C/Chl} \times 2^{\mu\text{maxC}} - \text{C/Chl} \quad (2)$$

Nitrate ([NO_3], micromolar) typically decreases with increasing temperature [*Harvey*, 1926; *Jackson*, 1983], and this relationship is variable with latitude [*Kamykowski and Zentara*, 1986; *Zentara and Kamykowski*, 1977]. We used the results of *Zentara and Kamykowski* [1977, Figure 2] to model the temperature-nitrate relationships in our computations. The intercepts in their work were originally estimated by eye (D. Kamykowski, personal communication, 1993), and we estimated the slope similarly. These relationships are summarized in Table 2. While this was sufficient for a global survey of this sort, a more precise estimate of the slope and intercept would be essential for a higher-resolution study.

To assess whether there was sufficient nitrate for the populations to maintain maximal nitrogen-specific growth (μ_{NO_3}), the Michaelis-Menten relationship was used [*Dugdale and Goering*, 1967]:

$$\mu_{NO_3} = \mu_{\text{maxN}} \times [S]/([S] + K_S) \quad (3)$$

where K_S was the half-saturation coefficient for nitrate uptake, and S was the nitrate substrate concentration. In order to apply the Michaelis-Menten model, realistic values of the nitrogen-specific maximum growth rate (μ_{maxN}) and half-saturation coefficient, which varied as a function of nitrate concentration, were needed. The two hyperbolic functions shown in (4) and (5) (see also Figure 2) showed good correspondence to field observations where at nanomolar nitrate concentrations in oligotrophic environments, the K_S was similar to the nitrate concentration and μ_{maxN} was low. At higher nitrate concentrations found in eutrophic environments, the K_S and μ_{maxN} increased toward a saturation value.

$$K_S = ([NO_3]/(3 + [NO_3])) \times 5.5 \quad (4)$$

$$\mu_{\text{maxN}} = ([NO_3]/(2 + [NO_3])) \times 3 \quad (5)$$

At each temperature, the maximum possible carbon-specific growth (μ_{maxC} from (1)) and the nitrate-specific growth rate (μ_{NO_3} in (3)) were compared, and the lesser was considered to be the maximum sustainable balanced growth rate μ_{maxbal}. This rate was converted to maximum "balanced carbon assimilation" using (2) (substituting μ_{maxbal} for μ_{maxC}). The model was run using several values of carbon/chlorophyll, θ,

Table 1. Sources of Pigment and Productivity Data Used in This Study

Data Set	Source*	Date	Location	Number of Stations
Biowatt	1	April 1984	North Atlantic	45
CalCOFI	2	May 1981 to April 1990	California Current	566
SCBS	3	Sept. 1974 to Jan. 1987	Southern California Bight	397
Fronts	2	July 1985	California Current	17
Med	4	May 1986	Mediterranean	19
SCOR	5	May–June 1970	Western Pacific/Caribbean	20
MARMAP	6	Aug. 1978 to June 1980	NW Atlantic shelf	1042
PRPOOS	1	Aug. 1985	Bermuda/Sargasso	8
TOGA/PRC	7	Jan.–Feb. 1986	Eastern Equatorial Pacific	139
Warm Core Rings	8	April–Oct. 1982	NW Atlantic	65
Global chlorophyll	9	1956–1982	global	4470
OCSAP	10	1958–1988	Subarctic Pacific	5443
Miscellaneous Atlantic	11	1973–1978	New York Bight	1170
North Sea	12	April 1980 to July 1986	North Sea	1430
GMEX	13	May 1964 to Sept. 1965	Gulf of Mexico	371
CABS	3	May and Oct. 1986, May and Oct. 1987	Southern California Bight	12
CAPEC	14	Jan.–Feb. 1973	coastal Portugal	74
CLIMAX	15	April 1968, Aug.–Oct. 1969	North and South Pacific	96
GOM	9	April and Aug. 1979, July 1980	Gulf of Maine	131
JGOFS	1	April–May 1989	North Atlantic	11
NOAA	16	Aug.–Sept. 1988	North Atlantic	36
Atlantis II	1	Dec. 1979 to Jan. 1980	South Atlantic	45
CF88	15	Aug.–Sept. 1988	North Pacific	18
Eastropac	3	Aug.–Sept. 1967, Apr. 1968	eastern tropical Pacific	176
Station P	17	March 1966 to Oct. 1967	Station P (50°N, 145°W)	121
Albatross	18	Dec. 1975, Feb. 1976	North Atlantic	141
Indian Ocean Expedition	19	Feb.–Aug. 1964	Indian Ocean	619
SUPER/miscellaneous	20	1978–1984	North Pacific	265
Merchant ship	21	March–Oct. 1990	South Pacific	477
INDEX/MONEX	22	March–July 1979	Somalian upwelling	37
Total				17,461

*Data sources are as follows: 1, J. Marra, Lamont-Doherty Earth Observatory, Columbia University, Palisades, New York. 2, T. Hayward, Marine Life Research Group, Scripps Institution of Oceanography (SIO), La Jolla, California. 3, R. W. Eppley, Food Chain Research Group, SIO. 4, S. Lohrenz, Center for Marine Science, University of Southern Mississippi, Stennis Space Center. 5, R. W. Austin, Center for Hydro-Optics and Remote Sensing, San Diego State University, San Diego, California. 6, J. E. O'Reilly, Sandy Hook Laboratory, NOAA National Marine Fisheries Service (NMFS), Highlands, New Jersey. 7, R. T. Barber, Duke University Marine Laboratory, Beaufort, North Carolina. 8, P. Wiebe, Woods Hole Oceanographic Institution, Woods Hole, Massachusetts. 9, C. S. Yentsch, Bigelow Laboratory, West Boothbay Harbor, Maine. 10, Results of Outer Continental Shelf Assessment Program, file 029 from the National Oceanographic Data Center (NODC), Washington, D. C. Data from the following groups and/or investigators are included: Institute of Oceanology, Hokkaido University (H. Koto and S. Motoda): University of Tokyo (R. Marumo, Y. Horibe, and T. Kuroki); Fisheries Research Board of Canada (J. D. H. Strickland, S. Tabata, L. Johnston, C. McAllister, D. G. Robertson, J. Meikle, A. Coombs, W. Atkinson, F. Dobson, R. Tripp, R. Tippet, H. Wilde, R. Stanley-Jones, J. Wong, K. Gantzer, D. Healey, C. Collins, B. G. Minkley, A. Dykes, C. De Jong, and J. Garrett), University of Washington (B. Frost, C. Lorenzen, R. Horner, C. Pautzke, G. Anderson, and W. Peterson), Biological Station at Nanaimo (T. R. Parsons and D. Fulton), U.S. Fish and Wildlife Service (J. McGary), University of Hawaii (R. Tsuda), SIO (J. McGowan and C. Miller), NMFS (J. Larrance), NOAA Pacific Marine Environmental Laboratory (A. J. Chester), University of Alaska (J. J. Goering, V. Alexander, and D. Schell), McNeese State University (D. Maples), Dames and Moore (G. Weissberg), C. Comiskey, Woodward-Clyde (K. Macdonald), and J. Vancil (no affiliations given). 11, File 049 of the NODC. Data of the following groups are included: City College of New York (T. Malone), Bigelow Laboratory (C. Garside), NMFS (J. Thomas), Skidaway Institute of Oceanography (J. Yoder). 12, P. Holligan, Plymouth Marine Laboratory, Plymouth, England. 13, S. el Sayed, Texas A&M University, College Station. 14, B. Saldanha, Instituto Hidrografico, Direccão do Servico de Oceanografia, Lisbon. 15, E. Venrick, Marine Life Research Group, SIO. 16, G. Hitchcock, Rosenstiel School for Marine and Atmospheric Science (RSMAS), University of Miami, Miami, Florida. 17, K. Stephens, Fisheries Research Board of Canada, Biological Station, Nanaimo, British Columbia, Canada. 18, T. J. Smayda, Graduate School of Oceanography, University of Rhode Island, Kingston. 19, M. Doty, Botany Department, University of Hawaii, Honolulu. 20, C. Lorenzen, School of Oceanography, University of Washington, Seattle. 21, Y. Dandonneau, Centre ORSTOM, Nouméa, New Caledonia. 22, S. Smith, Division MBF, RSMAS.

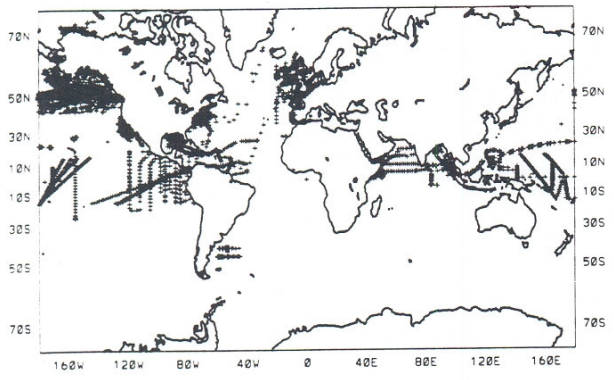

Figure 1. Geographic distribution of stations used in this analysis (n = 17,461).

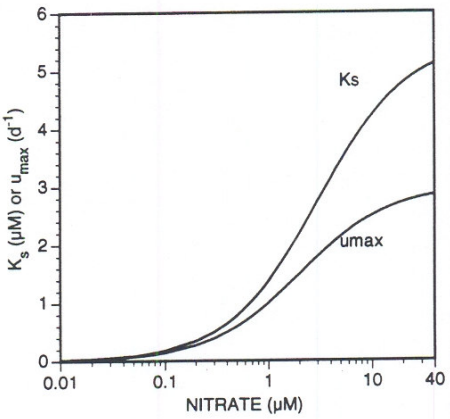

Figure 2. Curves describing K_S and μ_{maxN} based on nitrate concentration ((4) and (5), respectively).

as well as varying θ latitudinally as a function of temperature and light [*Geider et al.*, 1987]. To convert between carbon and nitrogen equivalents, the C/N ratio of 7 (by atoms) was used. No other nitrogen source (e.g., ammonium) was included in this model; thus μ_{NO_3} is representative of new production.

Baroclinicity Calculations

Several data sets were examined to verify whether gradients in SST were correlated to baroclinicity (here loosely defined as the slope of the isotherms in the top 200 m). Data from the Geochemical Ocean Sections Study (GEOSECS) [*Bainbridge*, 1980; *Craig et al.*, 1981; *Ostlund et al.*, 1987], the Indian Ocean Expedition [*Wyrtki*, 1971], Georges Bank [*Flagg*, 1987], and the equatorial Pacific [*U.S.-PRC TOGA (Tropical Ocean–Global Atmosphere) Program*, 1986, hereinafter referred to as TOGA] were used; for every station pair along the cruise tracks, an isotherm in the top 200 m was arbitrarily chosen and its slope was calculated. Of the available isotherms, if one remained in the top 200 m between two stations, it was preferentially used over isotherms that extended out of this surface layer. The gradient in SST between each pair of stations was also calculated.

Results

Prediction of Integrated Production and Ψ

In a purely empirical sense, one of the best predictors of integral production was P_m (milligrams C per cubic meter per day), the maximum production per unit volume within the euphotic zone. It explained 64% of the variance in integral production Π (using the notation of *Bannister* [1974] with units of grams C per square meter per day; $\log \Pi = 0.594 \times \log P_m - 1.15$; $r^2 = 0.64$; $n = 2859$; Figure 3). An even better predictor of integral production was P_m/K_{avg}, where K_{avg} was the average diffuse attenuation coefficient for photosynthetically active radiation (PAR) (in reciprocal meters) throughout the water column, based either on the secci depth or light measurements. This accounted for 73% of the variance in integral production ($\log \Pi = \log (P_m/K_{avg}) \times 0.70 + 0.25$; $r^2 = 0.73$; $n = 2118$; Figure 4). In our large data compilation, the average water column light utilization index Ψ [*Falkowski*, 1981] was 0.96 g C m^2 (g Chl Einstein^{-1} (Ein)), with 68% of the data falling between 0.4 and 2.3 g C m^2 (g Chl Ein)$^{-1}$ and 95% of the values falling between 0.2 and 5.4 g C m^2 (g Chl Ein)$^{-1}$. The Ψ data were log normally distributed. The strong empirical relationship between integral production and P_m/K_{avg} allowed for convenient calculation of Ψ by dividing P_m/K_{avg} by the product of integral chlorophyll I_{Chl} and incident light I_0 and taking their logarithms as shown in Figure 5. For 1248 stations, the best fit between directly measured Ψ and $P_m/(K \times I_{Chl} \times I_0)$ was $\log \Psi = (\log [P_m/K_{avg} \times I_{Chl} \times I_0]) \times 0.694 + 0.29$ ($r^2 = 0.75$).

Relationships Between Temperature and Nitrate, Nitrate-Dependent Growth, and Balanced Carbon Assimilation

There are significant latitudinal differences in the nitrate-temperature relationship. Our data base for nitrate and temperature was nowhere near as large geographically as those of *Zentara and Kamykowski* [1977] and *Kamykowski*

Table 2. Intercepts and Slopes of Temperature-Nitrate Relationships [*Zentara and Kamykowski*, 1977] Used To Predict Nitrate Based on Temperature as a Function of Latitude

Degrees of Latitude*	y Intercept, μM	Temperature of NO_3 depletion (x intercept), °C	Slope, μM/°C
60 to 69.99	33.0	4.5	−7.3
50 to 59.99	48.0	8.0	−6.0
40 to 49.99	180.0	9.0	−20.0
30 to 39.99	69.0	13	−5.3
20 to 29.99	70.0	14	−5.0
10 to 19.99	67.0	25	−2.7
0 to 9.99	49.2	27	−1.8
−10 to −0.01	46.7	28	−1.7
−20 to −10.01	60.0	21	−2.9
−30 to −20.01	55.0	18.5	−3.3
−40 to −30.01	77.3	14.5	−5.3
−50 to −40.01	54.6	14.0	−3.9
−60 to −50.01	66.7	7.5	−8.9

Predicted nitrate was constrained to the standard range found in seawater; it could go neither below 10 nM nor above 40 μM.

*Negative values indicate the southern hemisphere.

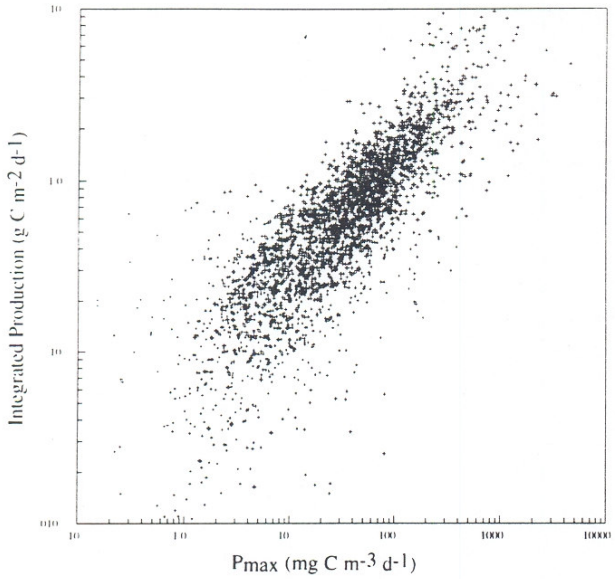

Figure 3. Relationship between integral production and P_{max} (both variables log transformed to produce normal distributions). P_{max} values represent maximum photosynthesis observed within the euphotic zone of a given station. Integral production values are integrated to the 1% light depth ($r^2 = 0.64$; $n = 2859$).

and Zentara [1986], although our limited data showed similar trends. The data of *Zentara and Kamykowski* [1977] clearly showed that as latitude increased, the temperature of nitrate disappearance decreased and the slope of the nitrate-temperature relationship increased (Table 2). It is known that nitrate concentrations in the ocean rarely fall below 0.01 μM [*Garside*, 1985]; thus any predicted nitrate concentration less than this value was reset to 0.01 μM. Similarly, maximal nitrate concentrations in the ocean rarely exceed 40 μM; thus if nitrate predicted by the equations in Table 2 exceeded this value, it was reset to 40 μM.

Applying a single nitrate-temperature relationship to the Michaelis-Menten model and the *Eppley* [1972] model showed that a plot of balanced carbon assimilation in the ocean versus temperature should have been highly nonlinear, not exponentially increasing as was observed for cultures [see *Eppley*, 1972, Figure 8]. An example of the temperature nitrate relationship for 20°–29.99° latitude is shown in Figure 6a, where nitrate was undetectable above 14°C. Using the relationships given earlier, the predicted K_S and μ_{max} versus temperature are also shown in Figure 6a. Figure 6b shows maximum growth predicted by *Eppley* [1972] and maximum growth predicted from the ambient nitrate concentrations, Michaelis-Menten kinetics, and associated coefficients. Assuming that the minimum of these two curves represents the maximum sustainable balanced growth, then the curve in Figure 6c results. Sensitivity analyses showed that decreasing the half-saturation coefficient for nitrate uptake allowed a higher rate of balanced growth at a given temperature. The greater the carbon:chlorophyll ratio, the larger the maximum balanced carbon assimilation that was sustained; varying θ with temperature and varying light as a function of latitude according to *Geider* [1987] did not change the overall shapes of the curves markedly (results not shown).

The above calculation was performed in 10° latitude increments between 60°N and 60°S. Temperature-nitrate relationships [*Zentara and Kamykowski*, 1977] and maximum balanced growth were predicted as a function of latitude (Figures 7a and 7b). The absolute highest P_b values

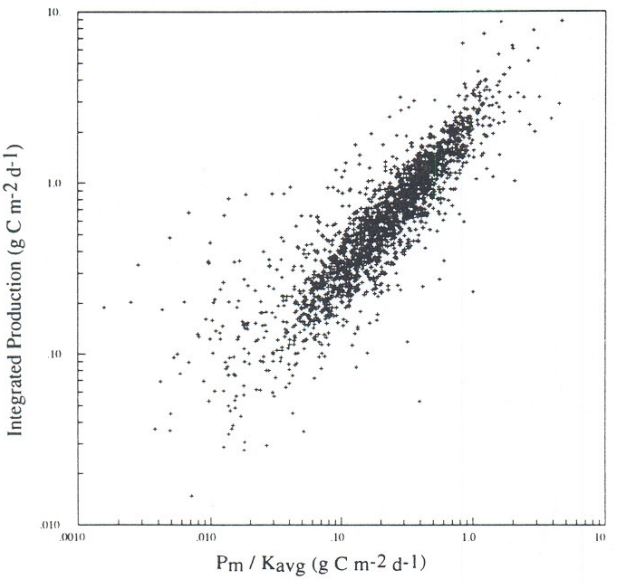

Figure 4. Relationship between integral production and P_{max}/K_{avg} (both variables log transformed to produce normal distributions). Integration depth was to the 1% light level ($r^2 = 0.73$; $n = 2118$).

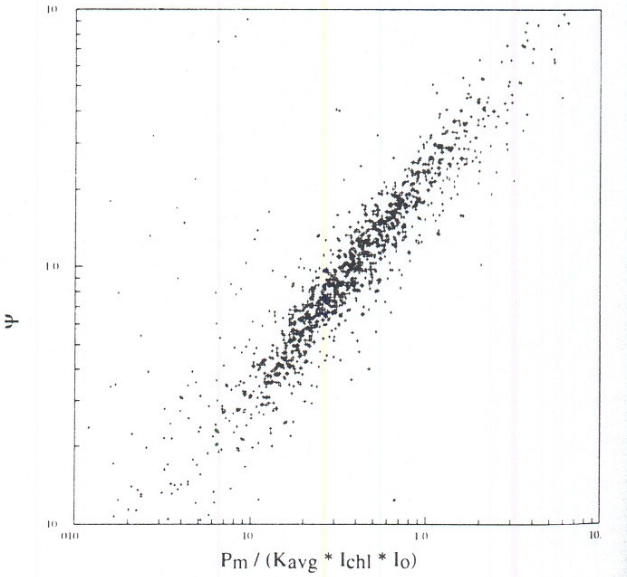

Figure 5. Estimation of Ψ, the water column light utilization index, from maximum photosynthesis, diffuse attenuation, integral pigment, and daily incident irradiance (PAR). Here, Ψ is defined as $\Pi/(B^*I_0)$, where B is integral biomass, and I_0 is daily incident irradiance. The data were log transformed to achieve normality ($r^2 = 0.75$; $n = 1248$).

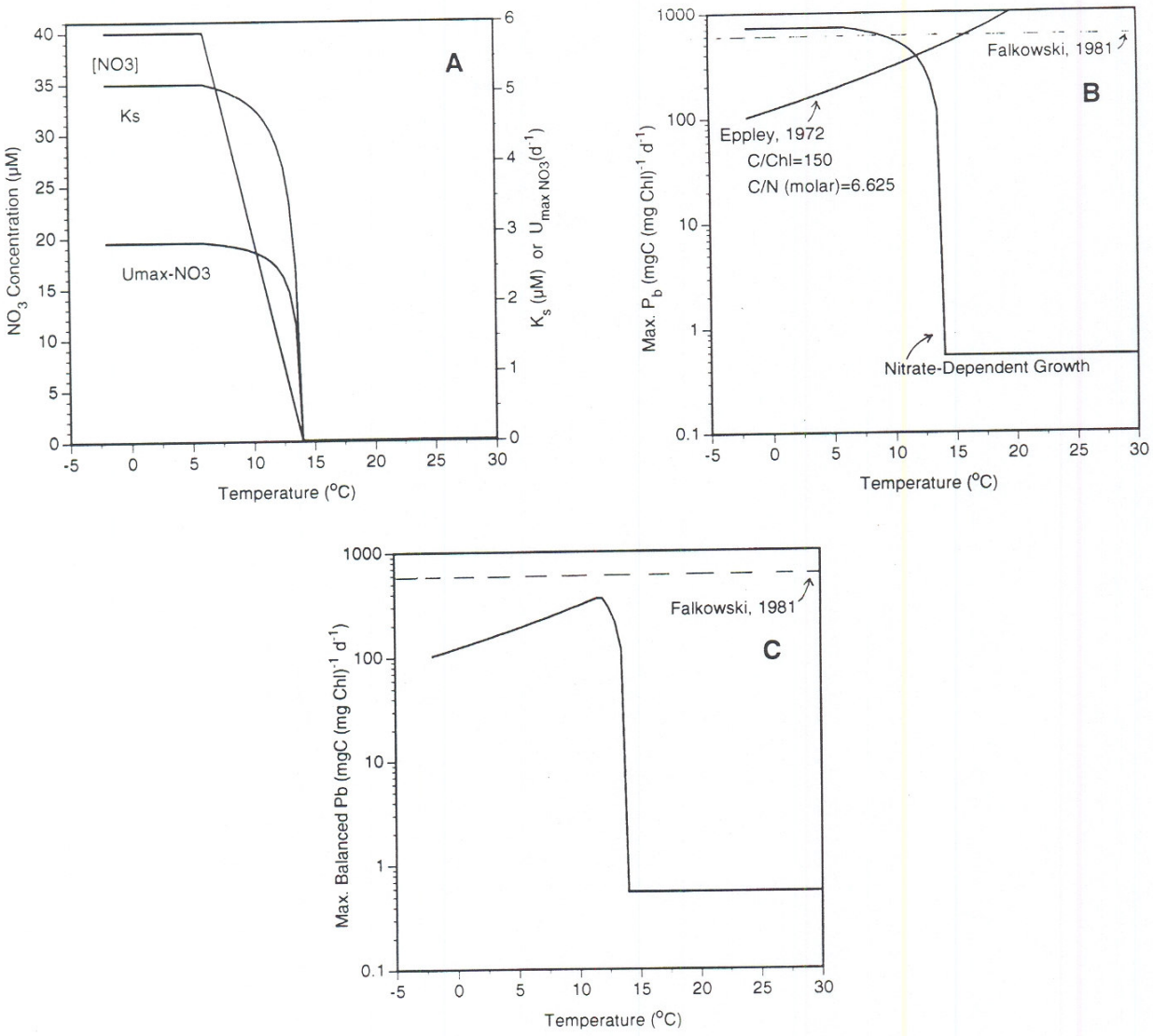

Figure 6. (a) Predicted nitrate-temperature relationship between 20°N and 29.99°N described by *Zentara and Kamykowski* [1977]. Right axis shows predicted Michaelis-Menten coefficients predicted from (4) and (5) (see also Figure 2). (b) *Eppley* [1972] relationship for maximum possible carbon assimilation as a function of temperature. The curve is based on (1) and (2) and assumes a carbon:chlorophyll ratio of 150 and a C/N ratio (molar) of 6.625. Also shown is the predicted nitrate-dependent growth based on Michaelis-Menten coefficients given in Figure 6a. This growth is given as carbon equivalents. The absolute maximum theoretical carbon assimilation that could be sustained under 24 hours of daylight is shown for reference (576 g C g Chl^{-1} d^{-1}). Obviously, a more reasonable theoretical maximum value for this latitude will be about half this value (300 g C g Chl^{-1} d^{-1}). (c) Maximum balanced C/N growth based on temperature and nitrate that can be sustained given the two curves in Figure 6b. Note the highly nonlinear nature of the function.

predicted by the model were in cool upwelled waters at the equator (about 400 g C g Chl^{-1} d^{-1}). At midlatitudes the absolute maximum P_b was less (about 300 g C g Chl^{-1} d^{-1}), and at boreal latitudes the value was about 250 g C g Chl^{-1} d^{-1}. In summary, the distinctly negative relationship between temperature and nitrate in the ocean combined with the *Eppley* [1972] temperature curve and the Michaelis-Menten hyperbola for growth as a function of nitrate [*Dugdale*, 1967; *Eppley et al.*, 1969; *Eppley and Thomas*, 1969] produced a "concave-down" curve for a plot of balanced growth versus temperature. Balanced growth rate increased as temperature increased up to some optimal temperature, above which nitrate limitation caused the maximum P_b to decline sharply.

Minimal turnover times of nitrate also were calculated on the basis of availability of nitrate and the maximum assimilation rate calculated above, assuming a Redfield ratio of carbon to nitrogen. No uptake of regenerated nitrogen was included in the calculation. Minimum nitrate turnover times were 40 days at ocean temperatures of ≦0°C, and this

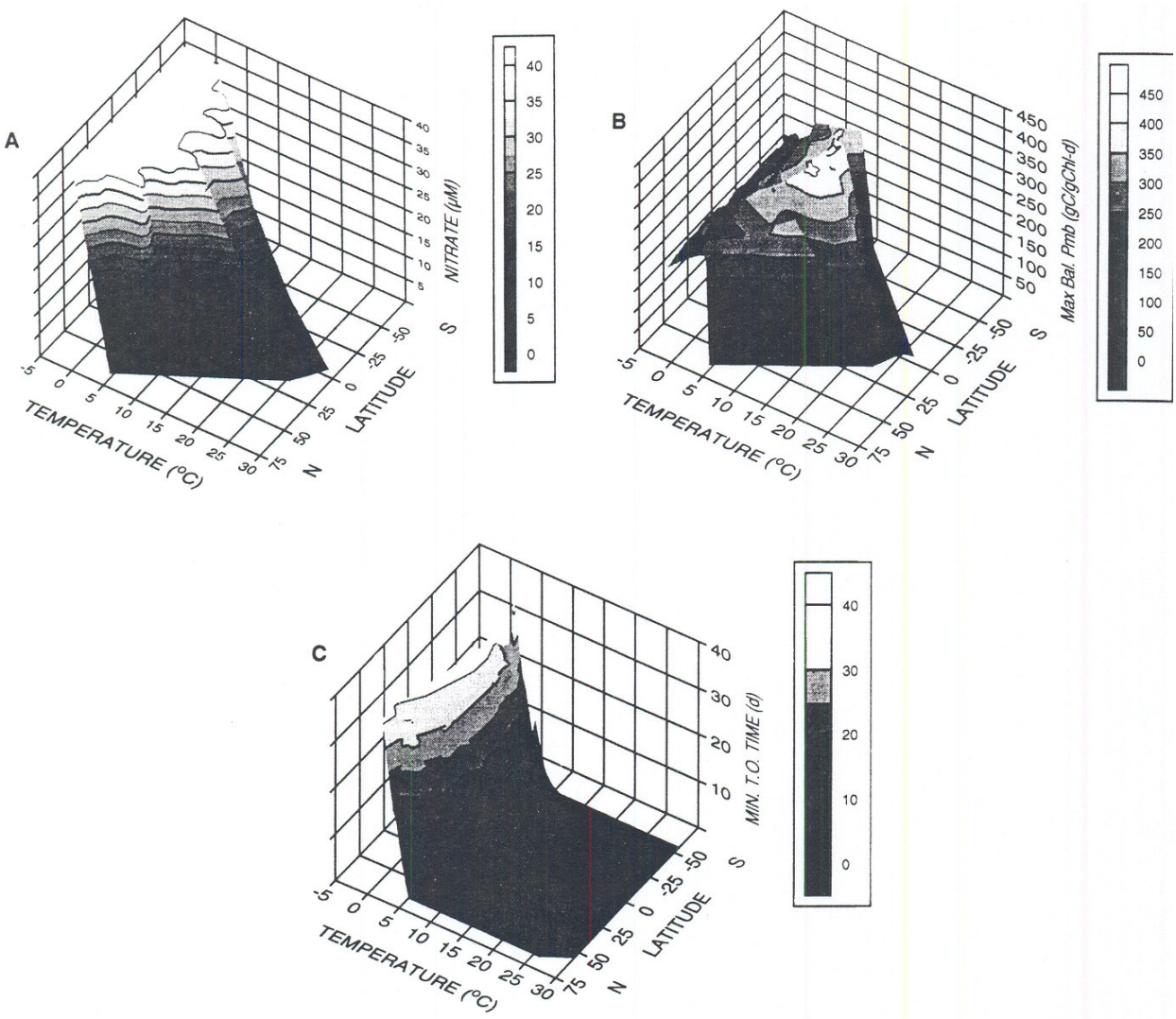

Figure 7. (a) Three-dimensional plot of nitrate-temperature relationships at various latitudes. This is a summary of the *Zentara and Kamykowski* [1977] relationships given in Table 2. (b) Maximum possible balanced carbon assimilation versus temperature at various latitudes. Contours are drawn at intervals of 50 g C g Chl^{-1} d^{-1}. Assumptions about C/Chl and C/N ratios are the same as those for Figure 6b. Carbon assimilation represents that which can be sustained by nitrate (using the Redfield ratio). (c) Minimum turnover time for nitrate based on the predicted nitrate concentration and the maximum possible balanced growth given in Figure 7b.

decreased sharply depending on latitude; above 15°C, the fastest nitrate turnover time was always less than 5 days (Figure 7c).

The predictions of the model were first compared to measured assimilation numbers regardless of latitude, plotted solely as a function of temperature and ignoring all light effects. Note that P_b, photosynthesis per unit biomass, was examined at all depths and light levels. Obviously, much of the variance of P_b at any one temperature was due to light-dependent effects which likely would have varied about 2 orders of magnitude throughout the euphotic zone at any single temperature. A plot of P_b versus temperature (degrees Celsius; Figure 8), with no pooling by latitude, showed the expected high scatter and no temperature dependence. These data were pooled in 2°C increments, and the number of data in each pool is shown in the lower panel of Figure 8. The highest P_b values, as indicated by the upper 95% confidence limits, varied between 100 and 300 g C g Chl^{-1} d^{-1}; however, it was generally rare in the entire data set to see assimilation numbers exceeding 200 g C g Chl^{-1} d^{-1} regardless of geographical location.

A somewhat different picture emerged when the data were pooled by latitude. To reduce the influence of single large values, the cutoff between the lower 95% and the upper 5% of the measured P_b data was calculated for each temperature range. As latitude increased, the relation between maximum P_b

and temperature steepened (Figure 9a). Below 30° latitude, the peak P_b values were much less than those at high latitudes. The same data are shown in three dimensions in Figure 9b.

Inferring the Isotherm Slope From the SST Gradient

The gradient in SST (G_{SST}; degrees per meter) was examined in several data sets against the slope of isotherms S_{iso} in the top 200 m of the water column. Figure 10 shows that for Atlantic and Pacific GEOSECS data [*Bainbridge*, 1980; *Craig et al.*, 1981; *Ostlund et al.*, 1987] and Indian Ocean data [*Wyrtki*, 1971], there was a well-defined inverse relationship between isotherm slope and SST gradient: $G_{SST} = (-24.37 \times S_{iso}) + 1.746 \times 10^{-5}$ ($n = 47$; $r^2 = 0.82$). These data spanned latitudes from the Antarctic convergence (55°S) to the Iceland-Faeroe Ridge (75°N). Six stations across the polar front had density dominated by salinity, and the isotherm depth gradients were an order of magnitude greater than those seen anywhere else. This severely biased the analysis, and these stations were excluded from Figure 10. The correlation between the SST gradient and the slope of the isotherms was found only at length scales greater than 250 km. An examination of a data set across Georges Bank with 20 km between stations [*Flagg*, 1987] showed no relationship between SST gradient and isotherm slope (not shown). Moreover, a line of 21 stations across the equatorial Pacific (165°E) with spacing of about 100 km showed no correlation between G_{SST} and S_{iso} [*TOGA*, 1986].

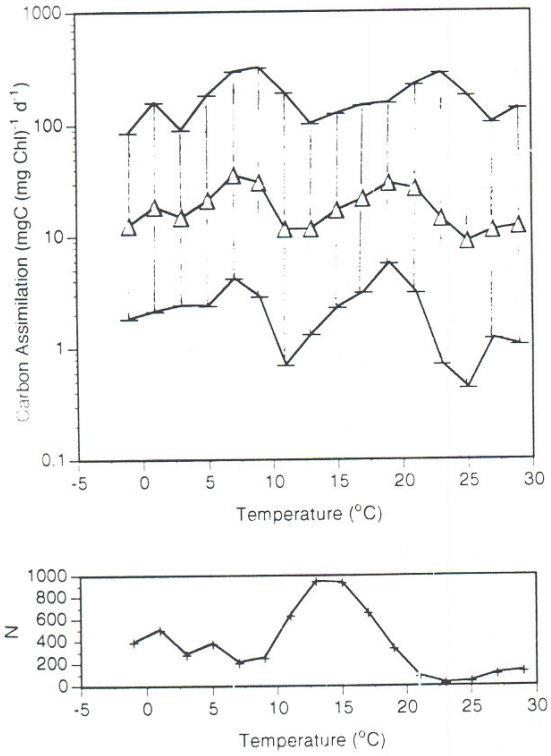

Figure 8. Temperature versus carbon assimilation statistics for 5286 measurements. Triangles represent the mean value for each 2°C increment. Error bars represent 95% confidence limits about each mean. Observations are from a wide variety of stations from equatorial to polar waters, mostly in the Atlantic and Pacific. Note that the ordinate is not P_m^b, the maximum photosynthesis normalized to chlorophyll, but P_b from all depths within the water column. Thus much of the variance in P_b at a given temperature was due to light-dependent effects. The bottom panel shows the number of data points in each mean.

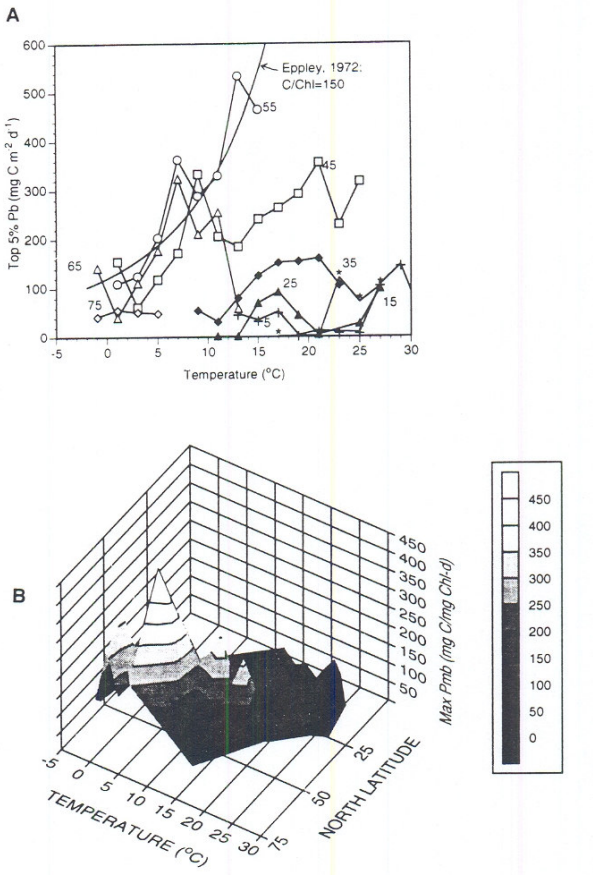

Figure 9. (a) Top 5% of P_b values versus temperature for 10° latitude increments: open diamond, 70°–80°N; open triangle, 60°–70°N; open circle, 50°–60°N; open box, 40°–50°N; solid diamond, 30°–40°N; solid triangle, 20°–30°N; plus sign, 10°–20°N; asterisk, 0°–10°N. Midlatitudes are shown to aid in viewing. *Eppley* [1972] curve for C/Chl ratio of 150 is shown for reference. (b) Three-dimensional representation of data given in Figure 9a.

Discussion

Relating P_m^b to Integral Production

It is clear from the results presented above that integral production is correlated to maximum photosynthesis of the water column (Figure 2) and is even better correlated to the maximum photosynthetic rate normalized to the average diffuse attenuation coefficient for the water column (Figure 3). There could be several possible reasons for this relationship. One must address the possibility of experimental error, though. For example, if there were interinvestigator differences in ^{14}C protocol (which is likely, given the wide variety of data sets that have been combined), covariance between

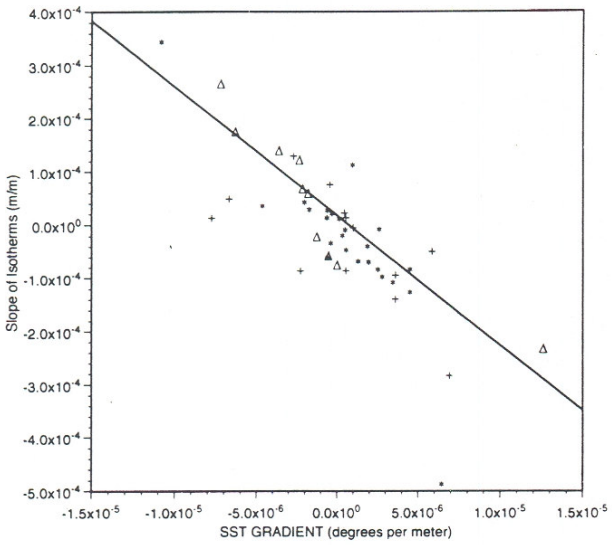

Figure 10. Slope of the isotherms in the top 200 m (S_{iso}) versus the gradient in sea surface temperature (G_{SST}). These data were from the Atlantic (asterisks) and Pacific (plus signs) GEOSECS cruises [*Bainbridge*, 1980; *Craig et al.*, 1981; *Ostlund et al.*, 1987] and Indian Ocean [*Wyrtki*, 1971; open triangles] covering latitudes from north of the Antarctic convergence to just south of the Iceland-Faeroe Ridge (excluding six stations poleward of the polar fronts, where density is dominated by changes in salinity). The data show a well-defined inverse relationship between the slope of the isotherms and the SST gradient at length scales of 250–500 km ($S_{iso} = -24.4 \times G_{SST} + 1.75 \times 10^{-5}$; $n = 47$; $r^2 = 0.82$).

integrated production and maximum production might have occurred. However, if this had been true, then the ratio between water column P_{max} and integral production would also have been highly variable, which was not the case. On average, P_{max} rates in 1 m^3 of water represented about 10% of the total integrated production (see the slope of the data in Figure 3). Although this seems to be an unusually large fraction of the total production (given that euphotic zones often range from 30 to 120 m), it implies that the depth range in which phytoplankton cells exhibit maximum photosynthesis is extremely narrow relative to the euphotic zone thickness. This is consistent with production being limited in the upper water column by photoinhibition or nutrient limitation and limited below by light limitation.

More intriguing is the relationship between the maximum photosynthesis normalized to the average diffuse attenuation coefficient K_{avg} (Figure 4). In this case our analysis of 2118 stations of data from a wide range of environments showed that log-transformed P_m/K_{avg} explained 73% of the variance in integrated production. Mechanistically, this is simplest to explain when the data are examined on linear instead of log axes. The average relationship between Π and P_m/K_{avg} can be approximated with

$$\Pi = (1.83 \times P_m/K_{avg}) + 0.26 \quad (6)$$

It is possible to tie this relationship to variability in the dimensionless ratio I'_0/I_k, the ratio of incident light just below the surface to the light level at which photosynthesis saturates. *Talling* [1957] used planimetry to show that there was a well-defined relationship between integral production and the ratio of P_m/K_m where K_m was the vertical extinction coefficient in the green region of the spectrum. He multiplied K_m by 1.33 to approximate light extinction values observed in the water types described by *Jerlov and Kullenberg* [1946] and *Jerlov* [1951]. Talling's relation for predicting integral production was given in his equation (7) (his product of primary production per unit population and population density is equivalent to P_m in our notation, i.e., photosynthesis per cubic meter per day; see his equation (3)):

$$\Pi = P_m \times [\ln 2/(1.33K_m)][(\log I'_0 - \log 0.5I_k)/\log 2] \quad (7)$$

where I'_0 is the light intensity just below the surface. If the logarithms in Talling's expression are simplified, K_{avg} is substituted for 1.33 K_m, and (7) is set equal to (6), then variation in I'_0/I_k can be seen as an inverse function of P_m/K_{avg}:

$$I'_0/I_k = 0.5(10^{(0.8+0.1K_{avg}/P_m)}) \quad (8)$$

The shape of this function is shown in Figure 11. The average P_m/K_{avg} ratio in the shipboard data was 0.25 (±1 standard deviation ranging from 0.10 to 0.62). Using Talling's model, this translated to an average I'_0/I_k of 7.9 (with ±1 standard deviation of 4.6 to 29.5). This is similar to the ratios of I'_0/I_k cited by *Platt and Sathyendranath* [1993] for 947 individual experiments (median of 7.2 with a range of 3.4 to 27) and a bit higher than their depth-averaged ratios of I'_0/I_k with a median of 5.7 and a range of 3.2 to 15. The greater range of these data was likely due to the larger geographic area sampled as well as to the diversity of investigators and techniques. Nevertheless, it is striking that the simple approximation of *Talling* [1957], when coupled to real measurements of water column maximum photosynthe-

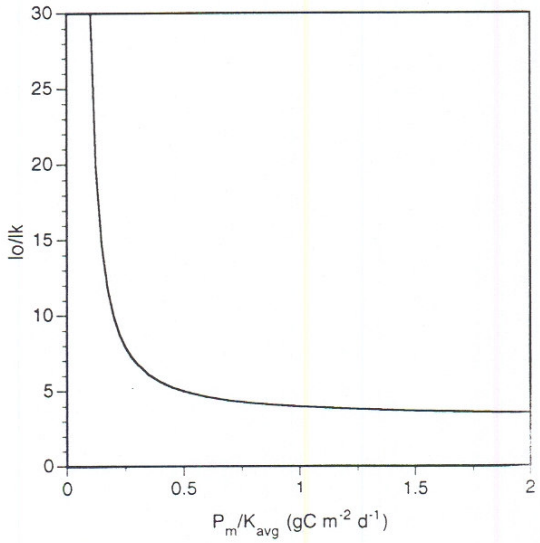

Figure 11. Predicted I'_0/I_k versus P_m/K_{avg} model using regression results from Figure 4 and model of *Talling* [1957]. The results show that the average value of I'_0/I_k estimated from the data set was 7.9 with confidence limits from 4.6 to 29.5 (±1 standard deviation).

sis and light extinction, produces average values of I'_0/I_k that are in good agreement with direct measurements of others.

Variability in Ψ

The values of Ψ showed more variability than expected [see *Platt*, 1986]. Nevertheless, such variance in Ψ was consistent with observations of *Malone* [1976] (Ψ of about 2.2 after conversion of his light data to PAR), *Falkowski* [1981] (average $\Psi = 0.43$), *Yoder et al.* [1985] (average $\Psi = 1.5$), *Campbell and O'Reilly* [1988] (average $\Psi = 1.47$), and *Balch et al.* [1989] (average $\Psi = 0.27$). It is likely that the water column light utilization index varies regionally, perhaps depending on species. However, it should be stressed that the variability we observed could have been caused by several experimental factors. Potential artifacts could have been caused by suboptimal incubation techniques (glass bottles, trace-metal-contaminated stocks, etc.) which would have lowered productivity values and hence Ψ. Large values of Ψ could have been due to underestimates of water column biomass (e.g., in a situation where the productivity maximum was above the 1% light depth and the deep chlorophyll maximum was below the 1% light depth, not included in the water column integration). Another way to explain high Ψ values might have involved how hourly production rates were converted to daily rates. Many data were originally given in units per hour and then multiplied by the day length to calculate the productivity per day. The respiratory component is difficult to calculate in these instances because of lack of knowledge about incubation time and dark-bottle subtraction. If no respiration were included, production values would have been overestimated, increasing Ψ. There are insufficient data to comment on the magnitude of the potential error in the light measurements, although this error also can be significant.

We addressed how large the errors would have to be to account for the total variance shown in Figure 5. In the simplest terms, if we hypothesize that Ψ was constant at 0.43 g C m^2 (g Chl Ein)$^{-1}$, then a value of $\Psi = 2$ g C m^2 (g Chl Ein)$^{-1}$ could have been explained by an error of about 450% in any one of the individual variables (positive error for integral production or negative error for chlorophyll or light). Such a value of Ψ also could have resulted from an error in two variables of about 65% (e.g., where production was 65% higher and light was 65% lower) or an error in all three variables such that integral production was 45% higher and both integral biomass and light were 45% lower. The largest error term was probably the productivity measurements, since the data were collected by many investigators using various techniques over many years. *Fitzwater et al.* [1982] estimated primary productivity using different techniques in oceanic and coastal waters. The mean productivity of samples incubated in polycarbonate bottles using clean ^{14}C stock was about 270–330% higher than the mean of samples incubated using the standard ^{14}C technique. Assuming error only in the productivity measurements, a value of $\Psi = 0.43$ made with the standard technique would translate to a value of 1.3 if clean techniques were employed. A respiration correction could increase this still further. Although our data suggest that Ψ is variable in the field, we cannot prove this with our data set, since error terms cannot be sufficiently quantified. The ramifications of a variable Ψ are important in a remote-sensing context, since it makes the determination of integral production more difficult, given inputs of integral biomass and light.

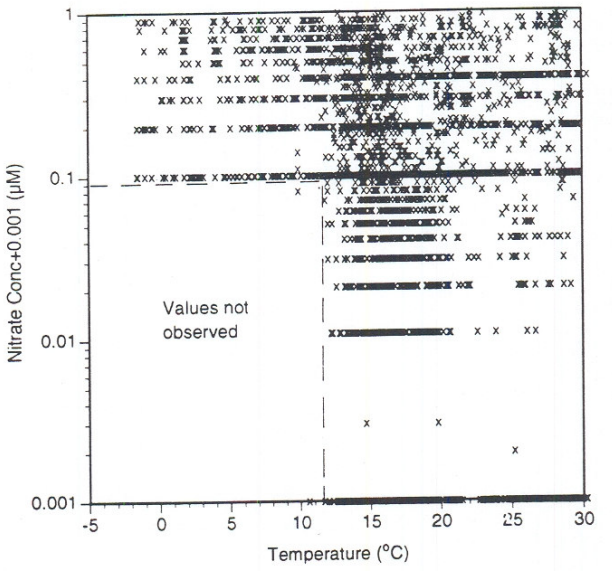

Figure 12. Scattergram of nitrate versus temperature at all latitudes showing lowest nitrate concentrations. Total size of nitrate-temperature data base is 15,150 measurements. Box represents region of scattergram where data are rarely observed.

A comparison between the abscissas of Figures 4 and 5 showed that the range of values for P_m/K_{avg} was similar to the range of $P_m/K_{\text{avg}} \times I_{\text{Chl}} \times I_0$, suggesting that the product of integral biomass and light was close to 1. This was fortuitous, however. The product of the mean integral biomass (grams Chl per square meter per day) and the mean surface irradiance (einsteins per square meter per day) indeed was about 0.7. However, there was no significant covariance between the two variables for 1248 stations examined.

Nitrate Versus Temperature Relationships

It is well known that the function relating nitrate concentration and temperature is a negative slope [*Zentara and Kamykowski*, 1977; *Kamykowski and Zentara*, 1986]. Equally important, though, are that (1) as latitude increases, nitrate disappears at progressively lower temperatures; and (2) the slope of the nitrate-temperature relationship decreases with decreasing latitude. In our compilation of nitrate data, regardless of latitude, undetectable nitrate was seen only at temperatures greater than about 12°C. Moreover, between −2° and about 12°C, the lowest nitrate ever observed in the 15,000-sample data set was about 0.1 μM (Figure 12). This may have been an artifact of the method for measuring nitrate, since at low temperatures, nitrate concentrations would have been higher and investigators may have used larger secondary standards for calibration, and this would have given coarser resolution at low concentrations. Nevertheless, given the size of the data set, it seems highly unlikely that there would have been no measurements made with the more sensitive calibration. This observation was interesting from an experimental point of view because, whether real or artifactual, it implied that there was little

evidence that phytoplankton in waters of 10°C or less could deplete nitrate below 0.1 μM. It would then follow that the algal half-saturation coefficients in these waters were greater than 0.1 μM. Although this was consistent with the interpretation that populations from warm, oligotrophic waters had lower half-saturation coefficients for nitrate uptake than populations from cool, eutrophic waters, this analysis should be repeated with the larger data sets such as the NODC data described by *Zentara and Kamykowski* [1977] and *Kamykowski and Zentara* [1986].

It was not surprising that with the variability in maximum P_b as a function of temperature, the shortest possible turnover time for nitrate also varied with temperature and latitude. For example, nitrate in high-latitude, 5°C surface waters would not be expected to turn over faster than about once per month because of slow growth rate and high nitrate concentrations. Any growth on regenerated nitrogen only will extend this turnover time, since ammonium will be taken up preferentially before nitrate [*McCarthy et al.*, 1975]. This is to be contrasted with 15°C water at midlatitudes, where the fastest that nitrate will be turned over is about once every 5 days, while at temperatures over 25°C near the equator, the minimum turnover time will be on a time scale of hours. The fact that the slope of the temperature-nitrate plots is more gradual at the equator also means that a mixing event at the equator will have a different impact than one near the poles. That is, provided nitrate is detectable, a 1° temperature decrease due to a mixing event will be associated with a greater upward nitrate flux at high latitudes. This, combined with slower growth at cold temperatures, means that the minimum time scale for depletion of a nitrate pulse will be longer at high latitudes.

Upper Limits to P_b as a Function of Temperature

The predicted maximum P_b values in Figure 7b are a highly nonlinear function of temperature and latitude. The results of our model runs showed that growth versus temperature relationship should have been identical to *Eppley*'s [1972] curve in cold waters (i.e., an exponentially increasing function) but in warm, nitrate-poor waters, growth should have become nitrogen limited and decreased as a function of temperature. The model also predicted that the response of balanced carbon assimilation to temperature should have been a function of the affinity of the cells for nitrate. That is, the lower the affinity, the more intense the nitrate limitation, and growth should deviate negatively from Eppley's line at progressively cooler temperatures. An unexpected result was that owing to the various temperature-nitrate relationships, the region that should sustain the highest absolute P_b values was near the equator. This was mainly because the slope of the temperature-nitrate relationship was the most gradual there and the temperature of "zero" nitrate was the highest.

Our model predictions were based on the Michaelis-Menten kinetics which incorporated lower half-saturation coefficients as ambient nutrients decreased (affinity increased as conditions became oligotrophic; see *Eppley et al.* [1969]). Moreover, the maximum saturated rates of uptake were assumed to be higher for eutrophic species. It is likely that over temporal scales of a day, the kinetic curves for nitrate uptake and growth were similar [*Eppley and Thomas*, 1969], even though it is well known that uptake velocities and growth rates may be highly different at short time scales, especially for ammonium uptake [*Goldman and Glibert*, 1983]. It was therefore implicit to the model that oligotrophic species dominated in low-nutrient waters owing to their higher affinity for nutrients, while eutrophic species dominated in high-nutrient waters owing to their higher maximal uptake and growth rates. Moreover, since changes in temperature were associated with changes in nitrate, one would expect maximum nitrate-specific growth to have increased as nitrate became more available in cold waters [see *Yentsch and Phinney*, 1989].

To compare the field results to model predictions, one must keep in mind that (1) errors in the ^{14}C measurements of different investigators undoubtedly varied over the 25 years that the data were collected (e.g., some of the highest assimilation numbers were flagged because either they exceeded the theoretical limit of 25 mg C (mg Chl h)$^{-1}$ cited by *Falkowski* [1981] (converted to daily rates) or they exceeded the maximum expected carbon-specific growth predicted by *Eppley* [1972] for their temperature and a maximum possible C/Chl ratio of 300 [*Steele and Baird*, 1962; *Eppley et al.*, 1977], (2) incubation temperature often did not match in situ temperature, (3) the productivity data were not evenly distributed across the temperature range −2° to 30°C (but note that any one temperature contained data from different regions and/or investigators), and (4) any P_b values reported in units of mg C (mg Chl h)$^{-1}$ were converted to mg C (mg Chl d)$^{-1}$ by calculating day length at a given latitude and calendar day, assuming that light varied as a sine function over the day [*Balch et al.*, 1992].

These factors notwithstanding, the shipboard data showed that the maximum P_b values predicted by Figure 7b were rarely attained in nature. When latitude was disregarded, maximum carbon assimilation was independent of temperature (Figure 8). However, when data were pooled by latitude, maximum carbon assimilation was positively correlated to temperature, especially in high-latitude, cooler water (Figure 9). The results from 55°N came the closest to the *Eppley* [1972] line, which suggests that the populations were minimally limited by factors other than temperature. This runs contrary to our expectations from the temperature-nitrate relationship at this latitude; nitrate should have been undetectable at temperatures of >8°–10°C, yet significant production was observed at temperatures up to 14°C. In the cases where the observed maximum P_b exceeded that predicted from (1)–(5), it could be argued that growth was based on regenerated nitrogen sources. This was also apparent from the fact that the highest measured P_b values at many other latitudes occurred at temperatures at which nitrate should have been low or undetectable. The only way to sustain this production (1) not balancing high P_b values by nitrogen uptake such that the C:N ratio of the particulate matter exceeded the Redfield ratio or (2) acquiring the extra nitrogen from the regenerated pool(s).

Some comments on the incubation conditions relevant to these results are in order. *Li* [1980] demonstrated a positive curvilinear relationship between assimilation number and growth temperature for cultures. The results showed that at higher temperatures the curve flattened and that between 20° and 30°C there was little increase in P_m^b. As Li pointed out, one should discriminate between assay temperature and growth temperature. Our data would reflect a combination of both types, because although the measurements were made in the field (close to the growth temperature), there may have

been incubator warming, which would have affected the assay temperature. It is impossible to discriminate between these two in this data compilation. Moreover, the differences between laboratory and field results may have been due to two additional factors. Field results obviously represented a continuum of species along a thermal gradient, not one species subjected to all different temperatures as in laboratory examples. Second, suboptimal assimilation numbers in the field may have resulted from suboptimal growth and incubation conditions.

Future Approaches for Estimating Primary Production Remotely

Possibility of Using Sea Surface Temperature to Indicate Baroclinicity

Our results indicated that regions in the ocean with large gradients in SST were regions with steep isopycnals (Figure 10). Stratified areas directly adjoining fronts have elevated production rates due to the combination of high nitrate concentrations from the deeply mixed side combined with reduced mixing on the stratified side of the front [see *Pingree et al.*, 1986, for more discussion on physical and biological effects of fronts]. In terms of remote sensing of primary production, this leads to the questions of whether SST gradients generally correlate to baroclinicity and whether SST gradients would relate to either the biomass or the productivity of the water column.

The baroclinicity versus SST relation appeared to be consistent between major ocean basins. Our analysis was confined only to temperature, since that is what can be measured by satellite. Thus the term "baroclinicity" was loosely used, since the slope of isotherms, not isopycnals, was examined. When crossing larger SST gradients into colder water (i.e., an increasingly negative SST gradient), the slope of the isotherms in the top 200 m steepened, rising more rapidly to the surface (Figure 10). Presumably, if salinity were also included, so that instead we could calculate density and plot true baroclinicity versus the surface gradient of density, the scatter would have lessened. Until we can predict salinity from space, we will have to settle for temperature as a proxy of density, however. The influence of salinity on the baroclinicity–SST gradient relationship was especially obvious in the GEOSECS data poleward of the polar fronts [*Bainbridge*, 1980; *Craig et al.*, 1981; *Ostlund et al.*, 1987].

Another aspect of this baroclinicity–SST gradient relationship was that it held at the mesoscale but not at smaller scales. The GEOSECS station spacing was on average about 250–500 km. Attempts to explore this relationship at scales of 20 km in the Gulf of Maine showed no significant correlation. It is logical to expect that the relationship would probably hold at length scales approximating the Rossby radius of deformation, but the baroclinicity–SST gradient relationship has yet to be tested over a sufficient continuum of station spacing. Whatever the scale, temperature and color imagery will likely have to be averaged at this threshold in order to relate baroclinicity to primary production.

Another area in which the SST gradient–baroclinicity relationship did not hold was across the equatorial Pacific at 165°E (10°N to 5°S; stations 29–51 of the TOGA expedition). This lack of relationship was not due to salinity being left out of the analysis, because the surface gradients in density also had no relation to the slope of the isopleth for $\sigma_t = 25$ (which usually was in the top 200 m), and the relation did not improve if the slope of the isopleth for $\sigma_t = 22$ was examined (which confined the baroclinicity measurements to the top 75 m). Perhaps most revealing of the dynamic nature of this region was that the slope of one isopycnal ($\sigma_t = 25$) was completely unrelated to the other ($\sigma_t = 22$). Wind-induced mixing was partially responsible for this, since SST was inversely correlated to the squared wind velocity (V_{wind} in meters per second; SST $= -0.079\ (V_{wind})^2 + 30.5$; $r^2 = 0.53$; $n = 22$). Again, the poor baroclinicity–SST gradient correlation was probably due to the large Rossby radius of deformation near the equator. This radius varies with the Coriolis force and hence with latitude. For example, it is almost 300 km at 4° latitude and 60 km at 18° latitude [e.g., *Chavez and Barber*, 1987]. It may be that the SST gradient–baroclinicity relationship will be usable only at mid to high latitudes.

Response of Phytoplankton to Changes in Baroclinicity

Even though the equatorial Pacific example given above did not show much correlation between integrated biomass or productivity and baroclinicity, there are regions of the world ocean that show distinct biological responses to increases in baroclinicity. *Yentsch* [1974, 1988] examined the relationship between σ_t at 100 m and integral biomass and found that the denser the water at 100 m, the greater the integral phytoplankton biomass. The relationship was different between the South Equatorial Current of the Atlantic and the Somali Current during the SW monsoon, apparently because of the different nitrate concentration associated with a given σ_t in these two regions [see *Kamykowski and Zentara*, 1986].

Steepness of isopycnals obviously is not the only factor dictating whether water mixes along density surfaces into the euphotic zone. Deriving a production estimate from baroclinicity will ultimately require some knowledge about the direction and rate of flow along isopycnals and the nitrate concentration at the base of the euphotic zone. Wind data may prove useful for inferring wind stress and wind stress curl and for calculating upwelling and downwelling rates [e.g., *Brock et al.*, 1991]. The importance of wind events in augmenting nutrients in the euphotic zone has been shown previously [e.g., *Walsh et al.*, 1978; *Glover et al.*, 1988; *Eppley and Renger*, 1988]. These workers make a strong case for using wind data to estimate the supply of nutrients for primary production.

Estimating Turnover Times of Carbon in Surface Waters

A final source of information which may aid in the prediction of primary production from space relates to the history of the algal populations in question. That is, by following a mesoscale population over time, one has a better idea of the stage of bloom development and whether growth terms outweigh loss terms or vice versa. This has been addressed on a CZCS pixel scale in the northeast Pacific [*Perry et al.*, 1989], where daily changes in pigment concentrations were used to infer total loss terms impacting the phytoplankton. Another example of using satellites to monitor the history of algal populations concerns coccolithophore blooms [*Balch et al.*, 1991]. It has been possible to estimate the beginning of these blooms using satellite imagery and then to use shipboard measurements to examine

variability in assimilation numbers and variability in cell morphology using microscopic enumeration of the populations. Decline of coccolithophore blooms as observed in satellite images has been verified in microscope counts and assimilation numbers [*Holligan et al.*, 1993]. Such observations reinforce the fact that two stations can have identical species, light, temperature, and pigment concentrations but very different assimilation numbers owing to nutrient limitation and senescence. Moreover, the decline of a bloom (as observed by satellite) may result from factors other than assimilation number, such as grazing.

Given that changes in satellite-derived biomass may not match the production predicted by *P-I* type algorithms, it may be possible to exploit this difference to advantage. In a best case scenario, a satellite estimate of surface production will approximate net daily production (gross photosynthesis minus algal respiration), because the *P-I* algorithms used with the satellite are based on bottle incubations; such incubations have no losses due to sinking, advection, or diffusion, and predation losses are confined to respiration and microzooplankton grazing. By confining primary production estimates to the top optical depth, the *P-I* type algorithms perform better than they do for integrated production estimates [*Balch et al.*, 1992]. The difference between a *P-I* type primary production estimate and the net change in biomass observed in two images over a day (Δ biomass day^{-1} based on assumed C/Chl) gives the first-order estimate of the total loss term. Dividing the surface standing stock by either the surface net production rate or the total loss term would allow approximation of the time scale of carbon turnover. Admittedly, such calculations will have error due to the precision of the surface pigment estimate, the assumed carbon:chlorophyll ratio, and the surface production estimate itself, but at least one is dealing with surface populations that can be observed directly by satellite and thereby can avoid error propagation due to modeling subsurface populations invisible to satellites.

Summary

This paper makes seven points based on the 17,000-station data compilation.

1. Empirical relationships for predicting integral production from shipboard estimates of P_m or P_m/K_{avg} are fairly robust (see Figures 3 and 4). The problem remains how to estimate K_{avg} and especially P_m from space. Although these empirical relations show promise, semianalytical formulations are ultimately preferred, provided they can account for the same or more variance in integral production. The values of P_m/K_{avg} combined with the model of *Talling* [1957] gave average values for I'_0/I_k of 7.9.

2. Water column light utilization index Ψ was predicted using shipboard values of P_m, K_{avg}, integral biomass, and light (which accounted for 75% of the variance in Ψ). The null hypothesis (Ψ is constant in nature) can be accepted only if large errors are invoked in the estimates of integral production, biomass, and light. There are insufficient data about the respective error terms to disprove the null hypothesis, although just using clean ^{14}C productivity techniques could increase Ψ by as much as 300%.

3. Over 15,000 nitrate analyses showed that between $-2°$ and 12°C, the lowest observed nitrate values were 0.1 μM, and "undetectable" nitrate was observed only above this temperature range. Whether this was an artifact or not, it means we have little evidence from which to conclude that phytoplankton in cold waters can assimilate nitrate to undetectable levels, which indirectly suggests higher nitrate affinity constants in cool waters.

4. Functions relating temperature to maximum carbon assimilation [*Eppley*, 1972], nitrate, and Michaelis-Menten growth kinetics were combined to predict maximum balanced carbon assimilation in 10° latitude bands. Model predictions showed that the upper limit to C/N assimilation should have a maximum at moderate temperatures within each latitude range. The highest possible P_b values would be expected in upwelling regions of the tropics.

5. Ship data from some 4200 stations divided into 10° latitude subsets showed that maximum P_b increased with temperature. The largest increase was observed at 55°N, close to the prediction of *Eppley* [1972]. Plots of maximum P_b versus temperature had lower slopes as latitude decreased.

6. Gradients in SST were related to the steepness of isotherms (a proxy for baroclinicity in many regions) at size scales of 250–500 km. The relationship degraded at smaller scales and lower latitudes, presumably because of regional differences in the Rossby radius of deformation.

7. Future estimation of carbon turnover from satellite data may be possible by comparing *P-I* type algorithms, which predict net production and usually do not include loss terms for sinking, advection, and large grazers, to changes in satellite-derived biomass over time, which incorporate all gain and loss terms. The difference between the two approximates the overall loss rate, which when divided into the biomass will approximate the time scale of carbon turnover.

Acknowledgments. We wish to acknowledge the many individuals who contributed the 17,500 stations of data. Kay Kilpatrick helped in the data entry, performed quality control of the data set, and reviewed an early draft of the manuscript. Several students helped in this data digitization effort: Shannon Cass, John Londono, Andrew Levy, Mark Moler (University of Miami Marine Sciences Program), and Rachel McGinnis (Bard College, New York). Elaine Collins of the National Oceanographic Data Center helped acquire some of the data sets used in this study (including the TOGA data set). Jim Postel and Rita Horner (University of Washington), D. Nebert and J. Goering (University of Alaska), and G. Heimerdinger, T. Piccilo, and Mike Crane (NODC) helped check sources of the NODC data. Hank Poor and Grant Basham solved many computer-related problems. Guillermo Podesta and Robert Evans helped in plotting Figure 1. This paper greatly benefitted from the discussion and comments of Richard Eppley, Patricia Matrai, Chris Garside, John Cullen, and Paul Falkowski. The comments of two anonymous reviewers are greatly appreciated. This work was generously supported by NASA (NAGW-2426).

References

Bainbridge, A. E., *GEOSECS Atlantic Expedition*, vol. 2, *Sections and Profiles, International Decade of Ocean Exploration*, 198 pp., National Science Foundation, Washington, D. C., 1980.

Balch, W. M., Reply, *J. Geophys. Res.*, *98*, 16,585–16,587, 1993.

Balch, W. M., M. R. Abbott, and R. W. Eppley, Remote sensing of primary production, I, A comparison of empirical and semi-analytical algorithms, *Deep Sea Res.*, *36*, 281–295, 1989.

Balch, W. M., P. M. Holligan, S. G. Ackleson, and K. J. Voss, Biological and optical properties of mesoscale coccolithophore blooms in the Gulf of Maine, *Limnol. Oceanogr.*, *36*, 629–643, 1991.

Balch, W. M., R. Evans, J. Brown, G. Feldman, C. McClain, and W. Esaias, The remote sensing of ocean primary productivity:

Use of a new data compilation to test satellite algorithms, *J. Geophys. Res.*, *97*, 2279–2293, 1992.

Bannister, T. T., Production equations in terms of chlorophyll concentration quantum yield, and upper limit to production, *Limnol. Oceanogr.*, *19*, 1–12, 1974.

Berry, J. A., and O. Bjorkman, Photosynthetic response and adaptation to temperature in higher plants, *Annu. Rev. Plant Physiol.*, *31*, 491–543, 1980.

Blackman, F. F., Optima and limiting factors, *Ann. Bot. 19*, 281–295, 1905.

Brock, J. C., C. R. McClain, M. E. Luther, and W. W. Hay, The phytoplankton bloom in the northwestern Arabian Sea during the southwest monsoon of 1979, *J. Geophys. Res.*, *96*, 20,623–20,642, 1991.

Campbell, J. W., and T. Aarup, New production in the North Atlantic derived from seasonal patterns of surface chlorophyll, *Deep Sea Res.*, *39*, 1669–1694, 1992.

Campbell, J. W., and J. E. O'Reilly, Role of satellites in estimating primary productivity on the northwest Atlantic continental shelf, *Cont. Shelf Res.*, *8*, 179–204, 1988.

Chavez, F. P., and R. T. Barber, An estimate of new production in the equatorial Pacific, *Deep Sea Res.*, *34*, 1229–1243, 1987.

Craig, H., W. S. Broecker, and D. Spencer, *GEOSECS Pacific Expedition*, vol. 4, *Sections and Profiles*, *International Decade of Ocean Exploration*, 251 pp., National Science Foundation, Washington, D. C., 1981.

Davison, I. R., Environmental effects on algal photosynthesis: Temperature, *J. Phycol.*, *27*, 2–8, 1991.

Dugdale, R. C., Nutrient limitation in the sea: Dynamics, identification and significance, *Limnol. Oceanogr.*, *12*, 685–695, 1967.

Dugdale, R. C., and J. J. Goering, Uptake of new and regenerated forms of nitrogen in primary productivity, *Limnol. Oceanogr.*, *12*, 196–206, 1967.

Dugdale, R. C., and F. P. Wilkerson, New production in the upwelling center at Point Conception, California: Temporal and spatial patterns, *Deep Sea Res.*, *36*, 985–1007, 1989.

Dugdale, R. C., A. Morel, A. Bricaud, and F. P. Wilkerson, Modeling new production in upwelling centers: A case study of modeling new production from remotely sensed temperature and color, *J. Geophys. Res.*, *94*, 18,119–18,132, 1989.

Eppley, R. W., Temperature and phytoplankton growth in the sea, *Fish. Bull.*, *70*, 1063–1085, 1972.

Eppley, R. W., and B. J. Peterson, Particulate organic matter flux and planktonic new production in the deep ocean, *Nature*, *282*, 677–680, 1979.

Eppley, R. W., and E. H. Renger, Nanomolar increase in surface layer nitrate concentration following a small wind event, *Deep Sea Res.*, *35*, 1119–1125, 1988.

Eppley, R. W., and W. H. Thomas, Comparison of half-saturation constants for growth and nitrate uptake of marine phytoplankton, *J. Phycol.*, *5*, 375–379, 1969.

Eppley, R. W., J. N. Rogers, and J. J. McCarthy, Half-saturation constants for uptake of nitrate and ammonium by marine phytoplankton, *Limnol. Oceanogr.*, *14*, 912–920, 1969.

Eppley, R. W., W. G. Harrison, S. Chisholm, and E. Stewart, Particulate organic matter in surface waters off southern California and its relationship to phytoplankton, *J. Mar. Res.*, *35*, 671–696, 1977.

Falkowski, P., Light-shade adaptation and assimilation numbers, *J. Plankton Res.*, *3*, 203–217, 1981.

Fitzwater, S. E., G. A. Knauer, and J. H. Martin, Metal contamination and its effect on primary production measurements, *Limnol. Oceanogr.*, *27*, 544–551, 1982.

Flagg, C. N., Hydrographic structure and variability, in *Georges Bank*, edited by R. H. Backus, pp. 108–124, MIT Press, Cambridge, Mass., 1987.

Gallegos, C. L., T. Platt, W. G. Harrison, and B. Irwin, Photosynthetic parameters of arctic marine phytoplankton: Vertical variations and time scales of adaptation, *Limnol. Oceanogr.*, *28*, 698–708, 1983.

Garside, C., The vertical distribution of nitrate in open ocean surface water, *Deep Sea Res.*, *32*, 723–732, 1985.

Geider, R. J., Light and temperature dependence of the carbon to chlorophyll *a* ratio in microalgae and cyanobacteria: Implications for physiology and growth of phytoplankton, *New Phytol.*, *106*, 1–34, 1987.

Glover, H. E., B. B. Prezelin, L. Campbell, M. Wyman, and C. Garside, A nitrate-dependent Synechococcus bloom in surface Sargasso Sea water, *Nature*, *331*, 161–163, 1988.

Goldman, J., and P. Glibert, Kinetics of inorganic nitrogen uptake by phytoplankton, in *Nitrogen in the Marine Environment*, edited by E. J. Carpenter and D. G. Capone, pp. 233–274, Academic, San Diego, Calif., 1983.

Gordon, H., and W. R. McCluney, Estimation of the depth of sunlight penetration in the sea for remote sensing, *Appl. Opt.*, *14*, 413–416, 1975.

Harrison, W. G., and T. Platt, Photosynthesis-irradiance relationships in polar and temperature phytoplankton populations, *Polar Biol.*, *5*, 153–164, 1986.

Harvey, H. W., Nitrate in the sea, *J. Mar. Biol. Assoc. U.K.*, *14*, 71–88, 1926.

Holligan, P. M., et al., A biogeochemical study of the coccolithophore *Emiliania huxleyi* in the North Atlantic, *Global Biogeochem. Cycles*, *7*, 879–900, 1993.

Jackson, G. A., The physical and chemical environment of a kelp community, in *The Effects of Waste Disposal on Kelp Communities*, edited by W. Bascom, 328 pp., Southern California Coastal Water Research Project, Long Beach, 1983.

Jerlov, N. G., Optical studies of ocean waters: Reports of the Swedish Deep-Sea Expedition, *Phys. Chem.*, *1*, 1, 1951.

Jerlov, N. G., and B. Kullenberg, On radiant energy measurements in the sea, *Sven. Hydrogr. Biol. Komm. Skr. Ny Ser. Hydrogr.*, *1*, 1, 1946.

Kamykowski, D., Some physical and chemical aspects of the phytoplankton ecology of La Jolla Bay, Ph.D. thesis, 269 pp., University of Calif., San Diego, 1973.

Kamykowski, D., and S. J. Zentara, Predicting plant nutrient concentrations from temperature and sigma-t in the upper kilometer of the world ocean, *Deep Sea Res.*, *33*, 89–105, 1986.

Li, W. K. W., Temperature adaptation in phytoplankton: Cellular and photosynthetic characteristics, in *Primary Productivity in the Sea*, edited by P. Falkowski, pp. 259–279, Plenum, New York, 1980.

Malone, T. C., Phytoplankton productivity in the apex of the New York Bight: Environmental regulation of productivity/chlorophyll *a*, in The Middle Atlantic Continental Shelf and New York Bight, edited by M. G. Gross, *Spec. Symp. Am. Soc. Limnol. Oceanogr.*, *2*, 260–272, 1976.

McCarthy, J. J., W. R. Taylor, and J. L. Taft, The dynamics of nitrogen and phosphorous cycling in the open waters of the Chesapeake Bay, in *Marine chemistry in the coastal environment*, *ACS Symp. Ser.*, *18*, edited by T. Church, 664–681, 1975.

Morel, A., and J. F. Berthon, Surface pigments, algal biomass profiles, and potential production of the euphotic layer: Relationships reinvestigated in view of remote-sensing applications, *Limnol. Oceanogr.*, *34*, 1545–1562, 1989.

Ostlund, H. G., H. Craig, W. S. Broecker, and D. Spencer, *GEOSECS Atlantic, Pacific and Indian Ocean Expeditions*, vol. 7, *Shorebased Data and Graphics*, *International Decade of Ocean Exploration*, 200 pp., National Science Foundation, Washington, D. C., 1987.

Perry, M. J., J. P. Bolger, and D. C. English, Primary production in Washington coastal waters, in *Coastal Oceanography of Washington and Oregon*, edited by M. R. Landry and B. M. Hickey, pp. 117–138, Elsevier, New York, 1989.

Pingree, R. D., G. T. Mardell, P. C. Reid, and A. W. G. John, The influence of tidal mixing on the timing of the spring phytoplankton development in the southern bight of the North Sea, The English Channel and on the northern American shelf, in *Tidal Mixing and Plankton Dynamics*, *Lect. Notes Coastal Estuarine Stud.*, *17*, edited by M. J. Bowman, C. M. Yentsch, and W. T. Peterson, pp. 164–192, Springer-Verlag, New York, 1986.

Platt, T., Primary production of the ocean water column as a function of surface light intensity: Algorithms for remote sensing, *Deep Sea Res.*, *33*, 149–163, 1986.

Platt, T., and A. Jassby, The relationship between photosynthesis and light for natural assemblages of coastal marine phytoplankton, *J. Phycol.*, *12*, 421–430, 1976.

Platt, T., and S. Sathyendranath, Oceanic primary production: Estimation by remote sensing at local and regional scales, *Science*, *241*, 1613–1620, 1988.

Platt, T., and S. Sathyendranath, Estimators of primary production

for interpretation of remotely-sensed data on ocean color, *J. Geophys. Res.*, *98*, 14,561–14,596, 1993.

Redfield, A. C., B. H. Ketchum, and F. A. Richards, The influence of organisms on the composition of seawater, in *The sea*, vol. 2, *The Composition of Sea Water: Comparative and Descriptive Oceanography*, edited by M. N. Hill, pp. 26–77, John Wiley, New York, 1963.

Riley, G. A., Factors controlling phytoplankton populations on Georges Bank, *J. Mar. Res.*, *6*, 54–73, 1946.

Sathyendranath, S., T. Platt, E. P. W. Horne, W. G. Harrison, O. Ulloa, R. Outerbridge, and N. Hoepffner, Estimation of new production in the ocean by compound remote sensing, *Nature*, *353*, 129–133, 1991.

Shuter, B., A model of physiological adaptation in unicellular algae, *J. Theor. Biol.*, *78*, 519–552, 1979.

Smith, R. C., R. W. Eppley, and K. S. Baker, Correlation of primary production as measured aboard ship in southern California coastal waters and as estimated from satellite chlorophyll images, *Mar. Biol.*, *66*, 281–288, 1982.

Smith, R. C., R. R. Bidigare, B. B. Prezelin, K. S. Baker, and J. M. Brooks, Optical characterization of primary productivity across a coastal front, *Mar. Biol.*, *96*, 575–591, 1987.

Steele, J. H., and I. E. Baird, Further relations between primary production, chlorophyll and particulate carbon, *Limnol. Oceanogr.*, *7*, 42–47, 1962.

Steemann Nielsen, E., Fertility of the oceans, in *The Sea*, vol. 2, *The Composition of Sea Water: Comparative and Descriptive Oceanography*, edited by M. N. Hill, pp. 129–164, John Wiley, New York, 1963.

Talling, J. F., The relative growth rate of three plankton diatoms in relation to underwater radiation and temperature, *Ann. Bot. London*, *19*, 329–341, 1955.

Talling, J. F., The phytoplankton population as a compound photosynthetic system, *New Phytol.*, *56*, 133–149, 1957.

U.S.-PRC TOGA (Tropical Ocean–Global Atmosphere) Program, Cruise and Data Report of USA-PRC joint air-sea interaction studies in the western tropical Pacific Ocean, *Contrib. 9*, 245 pp., Washington, D. C., 1986.

Walsh, J. J., T. E. Whitledge, F. W. Barvenik, C. D. Wirick, S. O. Howe, W. E. Esaias, and J. T. Scott, Wind events and food chain dynamics within the New York Bight, *Limnol. Oceanogr.*, *23*, 659–683, 1978.

Wilkerson, F. P., and R. C. Dugdale, The use of large shipboard barrels and drifters to study the effects of coastal upwelling on phytoplankton dynamics, *Limnol. Oceanogr.*, *32*, 368–382, 1987.

Wyrtki, K., *Oceanographic Atlas of the International Indian Ocean Expedition*, 531 pp., National Science Foundation, Washington, D. C., 1971.

Yentsch, C. S., The influence of geostrophy on primary production, *Tethys*, *6*, 111–118, 1974.

Yentsch, C. S., Why is primary productivity so high during the southwest monsoon? in *Marine Science of the Arabian Sea*, edited by M. G. Thompson and N. M. Termizi, pp. 349–358, American Institute of Biological Science, Washington, D. C., 1988.

Yentsch, C., and D. Phinney, A bridge between ocean optics and microbial ecology, *Limnol. Oceanogr.*, *34*, 1694–1705, 1989.

Yoder, J. A., L. P. Atkinson, S. S. Bishop, J. O. Blanton, T. N. Lee, and L. J. Pietrafesa, Phytoplankton dynamics within Gulf Stream intrusions on the southeastern United States continental shelf during summer 1981, *Cont. Shelf Res.*, *4*, 611–635, 1985.

Zentara, S. J., and D. Kamykowski, Latitudinal relationships among temperature and selected plant nutrients along the west coast of North and South America, *J. Mar. Res.*, *35*, 321–337, 1977.

W. M. Balch and C. F. Byrne, Division of Marine Biology and Fisheries, Rosenstiel School of Marine and Atmospheric Science, University of Miami, 4600 Rickenbacker Causeway, Miami, FL 33149-1098.

(Received February 8, 1993; revised November 1, 1993; accepted November 4, 1993.)